International Journal of Pharmaceutics 430 (2012) 228–237

Contents lists available at SciVerse ScienceDirect

International Journal of Pharmaceutics

journal homepage: www.elsevier.com/locate/ijpharm

Pharmaceutical Nanotechnology

Influence of precursor solvent properties on matrix crystallinity and drug release rates from nanoparticle aerosol lipid matrices

Amol Ashok Pawar[a], Da-Ren Chen[b], Chandra Venkataraman[a,*]

[a] Department of Chemical Engineering, Indian Institute of Technology Bombay, Mumbai, Maharashtra 400076, India
[b] Department of Energy, Environmental and Chemical Engineering, Washington University in St. Louis, St. Louis, MO, United States

ARTICLE INFO

Article history:
Received 3 January 2012
Received in revised form 16 March 2012
Accepted 16 March 2012
Available online 23 March 2012

Keywords:
Aerosol synthesis
Droplet evaporation
Lipid crystallinity
Anticancer drug

ABSTRACT

The crystallinity of drug-loaded lipid nanoparticles is believed to affect drug release rates; however, effective control over lipid crystallinity has not been achieved by current lipid nanoparticle preparation methods. The present study investigates control over the crystallinity of drug-loaded nanoparticle aerosol lipid matrices (NALM) through differences in evaporation rates of precursor solution drops and the subsequent control over drug release rates from these matrices. Gefitinib-loaded NALM were synthesized in an aerosol reactor using precursor solutions of gefitinib and stearic acid at a ratio of 1:4 w/w in organic solvents with high (dichloromethane) and low (ethyl acetate and chloroform) vapor pressures. Mean mobility diameter measured using a scanning mobility particle sizer was in the range of 123–132 nm with a unimodal distribution and a geometric standard deviation of 1.6–1.9. A layered particle structure was observed using transmission electron microscopy, which suggests partial drug enrichment in the surface layer. Higher drug loading (20% w/w) and uniform entrapment efficiencies (~100%) were achieved. The initial drug to lipid ratio (1:4 w/w) of the precursor solution was preserved in the synthesized lipid matrices. The crystallinity of the gefitinib-loaded lipid matrix was measured using X-ray diffraction and differential scanning calorimetry. In vitro drug release from gefitinib-loaded NALM in phosphate buffered saline (pH 7.2) over 10 days showed an initial fast release period followed by a prolonged sustained release period with varying release rates. Gefitinib-loaded NALM synthesized at higher evaporation rates exhibited lower degrees of crystallinity and faster drug releases. These results suggest the determinant role of lipid crystallinity manipulated by differing evaporation rates during aerosol synthesis on drug releases from nanometer-sized lipid matrices.

1. Introduction

Lipid nanoparticle matrices prepared from biocompatible lipids such as stearic acid and triglycerides have been explored for use in advanced drug delivery applications (Bunjes, 2010; Muller et al., 2000). Controlling the size, shape, and drug–lipid interactions of these matrices has been suggested to enhance drug bioavailability by tissue targeting and/or sustained release of encapsulated anticancer drugs (Patra et al., 2010; Wong et al., 2007). A particle-size governed enhanced permeation and retention effect of the lipid matrices loaded with anticancer drugs has been related to reduced toxicity, thereby improving drug specificity and efficacy (Wong et al., 2007). Moreover, particle size and shape govern the drug's specific surface area and diffusion distance, both of which are believed to affect drug release rates (Venkateswarlu and Manjunath, 2004; zur Muhlen et al., 1998). Drug–lipid interactions that arise because of the relative hydrophobicity or lipophilicity of the precursor lipids have been reported to affect solid lipid matrix viscosity, thereby influencing drug release rates (Muller et al., 2000; zur Muhlen et al., 1998).

Drug release rates from lipid matrices are also believed to be influenced by drug molecule diffusion rates through the lipid matrix and degradation rates of the matrix by enzymes such as lipases and esterases (Kheradmandnia et al., 2010; Muller et al., 2008; Olbrich et al., 2002b). Drugs that are immobilized in the solid crystalline lipid matrix exhibit lower molecular mobility than those in liquid lipids or supercooled melts (Kim et al., 2010; Uner and Yener, 2007; Westesen et al., 1997). Enzymatic degradation rates of lipid matrices have been reported to be slower for lipids with higher crystallinity (Olbrich et al., 2002a,b). The effect of degree of crystallinity on diffusing species in response to chemical potential gradients has been investigated for polymeric membranes and microparticles (Bitter, 1984; Jeong et al., 2003). Thus, lipid nanoparticle crystallinity could govern drug release rates.

Effective control over lipid nanoparticle crystallinity has not been achieved in current methods of preparing drug-loaded lipid

* Corresponding author. Tel.: +91 022 2576 7224, fax: +91 022 2572 6895.
E-mail address: chandra@iitb.ac.in (C. Venkataraman).

0378-5173/$ – see front matter © 2012 Elsevier B.V. All rights reserved.
doi:10.1016/j.ijpharm.2012.03.030

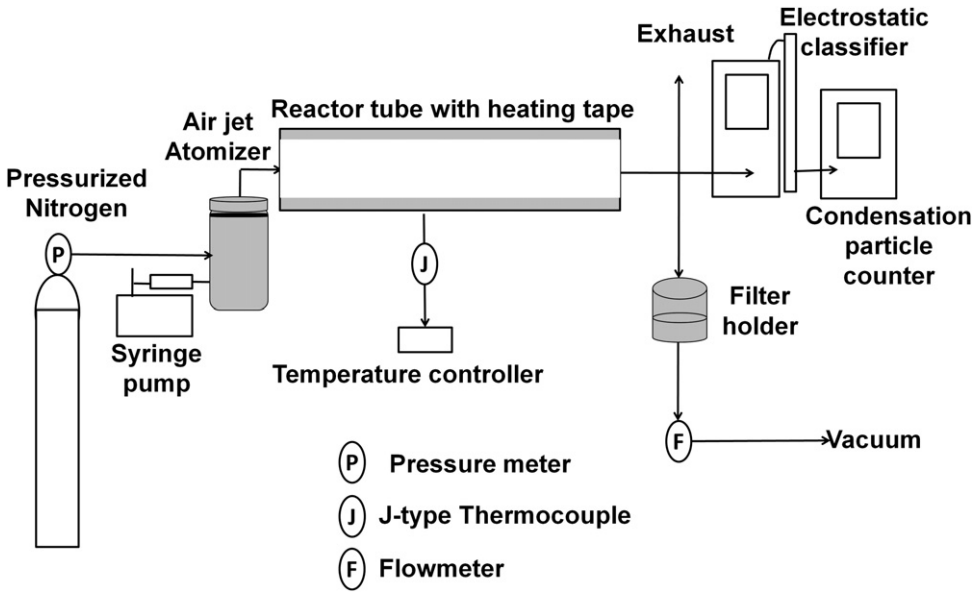

Fig. 1. Schematic diagram of the droplet-phase aerosol reactor for synthesis of gefitinib-loaded nanoparticle aerosol lipid matrices (NALM).

matrices, which primarily involve lipid melt-emulsification followed by high shear homogenization or ultrasonication (Bunjes, 2010; Mehnert and Mader, 2001). Drug-loaded lipid nanoparticles produced by these methods are reported to undergo characteristic crystalline polymorphic transitions that result in either burst release (100% drug release in less than 1 min) or drug expulsion during storage (Westesen et al., 1997). Crystallinity control was recently demonstrated in droplet-phase aerosol synthesis of stearic acid lipid nanoparticles with mean mobility diameters of 94–127 nm (Pawar and Venkataraman, 2011). Through a computational study, a lower measured degree of lipid crystallinity was related to a higher modeled droplet evaporation rate and a lower drop temperature resulting from evaporative cooling (Shetty et al., 2011). The influence of the difference in lipid crystallinity on drug release rates is of interest. Therefore, this study focuses on investigating drug release rates of the anticancer drug gefitinib (Iressa®) from stearic acid lipid matrices of varying lipid crystallinities. Stearic acid is solid under temperatures of application (room and physiological conditions), with a well-understood crystalline structure, allowing the study of changes in this property from the influence of aerosol synthesis conditions. Among other crystalline lipids, triglycerides including trimyristin, tripalmitin and tristearin, have been used to synthesize lipid nanoparticles (Mehnert and Mader, 2001), largely through lipid melt emulsification. These exhibit lower crystallization tendencies and presence of unstable polymorphic states (Bunjes, 2010; Bunjes et al., 1996), whose transformations during storage could expel encapsulated drug (Mehnert and Mader, 2001). Gefitinib, which is prescribed for the treatment of lung, pancreatic, and breast cancers, was selected as a model hydrophobic drug. Gefitinib inhibits selective cancer cell-surface epidermal growth factor receptors and consequently activates cancer cell apoptosis (Cohen et al., 2003). Many hydrophobic anticancer drugs, including gefitinib and paclitaxel, have poor aqueous solubility and poor bioavailability. Encapsulating such poorly water soluble compounds within lipid nanoparticles has been reported to improve their dissolution, targeting, and subsequent bioavailability (Bunjes, 2010; Chakraborty et al., 2009). Among the drugs considered, the Biopharmaceuticals Classification System (BCS) classification of gefitinib is II, indicating that it has greater permeability than paclitaxel, whose BCS classification is IV, implying the superior absorption properties of gefitinib into body tissues (Bergman et al., 2007). The specific objectives of the present work are to investigate the following:

1. Effect of drug (gefitinib) incorporation on the crystalline properties of stearic acid lipid nanoparticles synthesized under controlled evaporation via the droplet-phase aerosol route
2. Drug release rates from gefitinib-loaded stearic acid nanoparticles

2. Materials and methods

2.1. Experimental approach

Stearic acid lipid matrices synthesized using the droplet-phase aerosol synthesis method were termed nanoparticle aerosol lipid matrices (NALM) (Pawar and Venkataraman, 2011). Thus, in the present study, gefitinib-loaded NALM were synthesized using the same method and are hereafter referred to as "gefitinib-loaded NALM." The experimental system used for the synthesis of gefitinib-loaded NALM (Fig. 1) comprised an indigenously designed aerosol reactor, collision-type air jet atomizer (Model 3076; TSI Inc. Particle Instruments, St. Paul, MO, USA), scanning mobility particle sizer (SMPS; Model 3936; TSI Inc. Particle Instruments), and a filter assembly and a micro-orifice uniform deposit impactor (MOUDI, Model No. 110; MSP Corp., Shoreview, MN, USA). The precursor solution was fed into the air jet atomizer with a syringe pump (PHD 2000; Harvard Apparatus, Holliston, MA, USA). Details of the aerosol reactor were described previously (Pawar and Venkataraman, 2011). Samples for the drug incorporation and release measurements were collected on 25-mm glass-fiber filters in a filter holder (Millipore, Billerica, MA, USA), whereas samples for mass distribution and crystallinity measurements were collected on the MOUDI cascade impactor.

Control over evaporation rates during droplet-phase aerosol synthesis was achieved through selection of precursor solvents with varying vapor pressures including ethyl acetate (ETA), chloroform (CHL), and dichloromethane (DCM) (>99.0% pure; Sigma–Aldrich, St. Louis, MO, USA). The calculated vapor pressures of ETA, CHL, and DCM at 298 K were 12,524 Pa, 25,729 Pa, and 56,927 Pa, respectively. Pure gefitinib nanoparticles were synthesized using a gefitinib precursor solution (1 mg/mL) dissolved

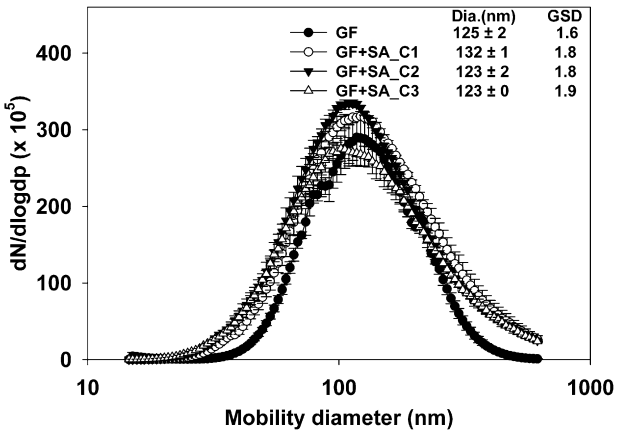

Fig. 2. Number size distributions of pure gefitinib nanoparticles (GF) and gefitinib-loaded nanoparticle aerosol lipid matrices (NALM) with crystallinity C1, C2, and C3 in descending order synthesized using gefitinib and stearic acid (1:4 w/w) solutions of ethyl acetate (ETA), chloroform (CHL), and dichloromethane (DCM), respectively.

in ETA. Precursor solutions (1 mg/mL) used for the synthesis of gefitinib-loaded NALM were prepared by dissolving gefitinib (Thermo Fisher Scientific Inc., Barrington, IL, USA) and stearic acid (95% pure; Sigma–Aldrich) at a 1:4 w/w ratio in the selected solvents. The precursor solution (20 mL) was charged in a 20-mL syringe, loaded in a syringe pump, and delivered at 1.2 mL/min. The atomized droplets were entrained in a nitrogen flow at 3 L/min through an aerosol reactor. Atomization was conducted for 40 min, during which time SMPS scans of the particle mobility distributions and sampling were performed.

2.2. Measurement of particle size

Real-time number size distributions, based on electrical mobility diameter, were measured using SMPS equipped with a differential mobility analyzer (Long DMA, Model 3081; TSI Inc. Particle Instruments) and a condensation particle counter (CPC, Model 3075; TSI Inc. Particle Instruments). The relative standard deviations of the three measurements in each size bin of the SMPS output in the mobility diameter range of 14–660 nm (Fig. 2) were 1–30%.

The size-fractionated samples collected in MOUDI were subjected to gravimetric analysis to obtain the aerodynamic mass distribution. Pre-cleaned, -dried, and -weighed aluminum foils (0.027-mm thick, 45 mm in diameter) were used as substrates for the gravimetric collection. Aluminum foils were conditioned at 298 K and 40–50% relative humidity (RH; air-conditioned room) for 15 h prior to weighing both before and after sample collection. The nominal uncertainty in total mass collected on MOUDI was 5–6% from three repeat experiments. The samples were stored in airtight containers in an air-conditioned room at 298 K. The humidity in the room during sample storage was measured using a digital hygrometer (TEMPTEC, Mumbai, India) and found to be in the range of 40–50% RH.

2.3. Shape and internal structure of gefitinib-loaded NALM

The sizes and shapes of gefitinib-loaded NALM were examined using transmission electron microscopy (TEM, Technai G2; FEI, Hillsboro, OR, USA) and scanning electron microscopy (SEM, Nova NanoSEM 2300, FEI, Hillsboro, OR, USA). Gefitinib-loaded NALM collected on glass-fiber filters were transferred to the lighter side of Formvar-coated copper grid (Pelco®, TedPella Inc., Redding, CA, USA). Uranyl acetate solution (2% w/v) (Electron Microscopy Sciences, Hatfield, PA, USA) in 0.1 M aqueous sodium cacodylate buffer (pH 7.3) was used as a negative staining solution. Using a micropipette, 20 μL of the staining solution filtered through a 220-nm filter was dropped over the grid placed in a Petri dish. The excess solution was absorbed using lint-free filter paper. The sample was then dried overnight and observed under TEM at an accelerating voltage of 120 kV.

SEM was used to examine the surface features of gefitinib-loaded NALM collected on glass-fibre filters that were transferred onto SEM stubs. To improve the sample electrical conductivity, sample-containing SEM stubs were coated with gold by low vacuum (0.05 atm) sputtercoating for 3 min. After the gold coating was complete, the samples were observed under SEM at an accelerating voltage of 10 kV.

2.4. Measurement of particle crystallinity

The prepared NALM were subjected to crystallinity measurements using powder X-ray diffraction (PXRD; Model X'Pert Powder, PANalytical Ltd., EA Almelo, the Netherlands) and differential scanning calorimetry (DSC; Model Pyris 6 DSC, PerkinElmer Inc., Waltham, MA, USA) as well as comparison with bulk stearic acid and a bulk mixture (1:4 w/w) of bulk gefitinib and stearic acid. PXRD patterns (diffractograms) were measured by an X-ray diffractometer operating in the Bragg–Brentano geometry equipped with an X'Celerator detector (PANalytical Ltd.), a copper radiation source, and a secondary monochromator operating at 40 kV and 30 mA. The diffraction measurements were made at 298 K over a scattering angle (2θ) range of 3–30 using steps of 0.02 2θ and 10 s scan step time. Peak area profiling and determination at specific 2θ diffraction angles were performed using HighScore Plus software (PANalytical Ltd.) and was compared with that of the International Centre for Diffraction Data standard for stearic acid.

Melting enthalpy and melting point analyses were performed using DSC. Prior to the thermal analysis, the instrument was calibrated with indium (calibration standard, purity >99.999%). For thermal analysis, ~2 mg of the lipid samples was weighed in standard aluminum sample pans (40 μL) that were then hermetically crimped. An empty standard aluminum pan was used for reference. DSC thermograms of the samples were recorded at a heating rate of 293 K/min under a nitrogen purge (20 mL/min) in a temperature range of 303–503 K corresponding to the melting point range of different stearic acid crystalline forms and gefitinib. The melting points and enthalpies were calculated using Pyris™ software (PerkinElmer Inc.). Following earlier studies (Venkateswarlu and Manjunath, 2004), percentage crystallinity of NALM was calculated as a ratio of their measured melting enthalpies to that of bulk mixture, assuming that the latter corresponded to the energy needed for fusion from a 100% crystalline state.

2.5. Measurement of drug incorporation efficiency

To determine drug incorporation efficiency, ~3–5 mg of gefitinib-loaded NALM collected on glass-fiber filters was immersed in a 20-mL glass vial containing 10 mL of dimethyl sulfoxide (DMSO; >99.6% pure; Sigma–Aldrich) for 15–20 min with gentle shaking. The gefitinib concentration was determined using high-performance liquid chromatography (HPLC) equipped with an autosampler, binary pump, temperature-controlled column compartment, and a variable wavelength detector (1100 Series System; Agilent Tech, Santa Clara, CA, USA). A 4.6 × 150 mm Zorbax SB-C18 3.6-μm column was used and the detection wavelength was fixed at 348 nm. A gefitinib calibration curve was prepared using DMSO solutions with varying gefitinib concentrations (2.5, 5, 10, 20, 40, and 80 μg/mL) along with stearic acid (100 μg/mL). The mobile phase comprised of 0.05 M aqueous ammonium acetate (99.99%; Sigma–Aldrich) and acetonitrile (>99.9%; Sigma–Aldrich) at a 20:80 v/v ratio. The flow rate of the mobile phase was maintained

at 1 mL/min. Drug incorporation efficiency was expressed both as drug loading (% w/w) (referred to as drug content in the literature) and drug entrapment (% w/w), calculated using Eqs. (1) and (2), respectively:

$$\text{Drug loading}\,(\%\,\text{w/w}) = \frac{\text{mass of drug in NALM}}{\text{mass of NALM recovered}} \times 100 \quad (1)$$

$$\text{Drug entrapment}\,(\%) = \frac{\text{mass of drug in NALM}}{\text{mass of drug in precursor solution}} \times 100 \quad (2)$$

2.6. Measurement of in vitro drug release

For the drug release studies, ~3–5 mg of pure gefitinib nanoparticles and gefitinib-loaded NALM collected on glass-fiber filters were immersed in 1 mL of release medium (phosphate buffered saline [PBS], 1×, pH 7.4 ± 0.2, without calcium and magnesium; Mediatech Inc., Manassas, VA, USA), in a 1.5-mL sample tube. This sample tube was then kept on an orbital shaker under continuous gentle mixing (Nutator Mixer, Model No. 421105; TCS Scientific Corp., New Hope, PA, USA) at 298 K. One milliliter of release medium containing released drug was withdrawn at scheduled time intervals without disturbing the immobilized NALM in the filter. Fresh release medium was immediately added to the sample tube after each sample was removed. The samples obtained at regular intervals were used to measure the released drug concentration using HPLC. A plot of the cumulative percent release vs. time was drawn using area under the peak at the retention time for gefitinib at 6–7 min of elution.

2.7. Statistical analysis

The data are presented with mean values ± standard deviation for three replicates for each experimental set. The statistical significance of the differences was evaluated using Student's *t*-test and values of $p < 0.05$ were considered statistically significant.

3. Results and discussion

Particle size, shape, internal structure, and lipid crystallinity are properties of interest that influence drug release rates from lipid matrices. Gefitinib-loaded NALM were synthesized in the aerosol reactor at varying evaporation rates using precursor solutions of gefitinib and stearic acid dissolved at a 1:4 w/w ratio in the selected solvents with differing vapor pressures. The particle properties of pure gefitinib nanoparticles and gefitinib-loaded NALM were then studied to investigate the effect of lipid crystallinity on drug release rates.

3.1. Size distribution of gefitinib-loaded NALM

In the present study, median mobility diameters of pure gefitinib nanoparticles and gefitinib-loaded NALM aerosols (Fig. 2) were in the range of 123–132 nm, with reasonably narrow unimodal size distributions (geometric standard deviation [GSD] of 1.6–1.9). A concentration of ~10^6 particles/cm^3, similar to that of the generated droplets (TSI 2008), indicates the formation of one particle per drop with negligible coagulation or drop fragmentation. The MOUDI-derived aerodynamic size distributions of gefitinib-loaded NALM aerosols (Fig. 3) had a mass median aerodynamic diameter of 368–412 nm with a GSD of 1.9. The differences in the NALM aerosol properties, like median diameter, which were based on both mobility and aerodynamic behavior, were not statistically significant ($p > 0.05$). Therefore, the size distributions of gefitinib-loaded NALM aerosols synthesized at varying evaporation rates were relatively invariant.

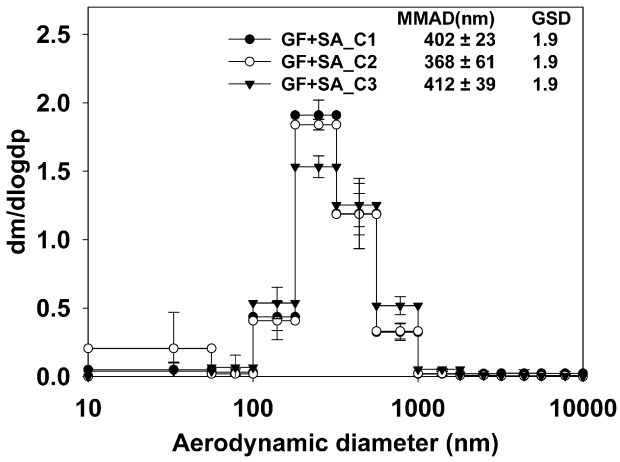

Fig. 3. Mass size distributions of gefitinib-loaded nanoparticle aerosol lipid matrices (NALM) with crystallinity C1, C2, and C3 in descending order synthesized using gefitinib and stearic acid (1:4 w/w) solutions of ethyl acetate (ETA), chloroform (CHL), and dichloromethane (DCM), respectively.

3.2. Shape and internal structure of gefitinib-loaded NALM

Gefitinib-loaded NALM synthesized at varying evaporation rates and observed under both TEM and SEM were spherical in shape and had particle diameters of ~100–200 nm (Figs. 4–5). In the SEM images, gefitinib-loaded NALM exhibited smooth surface properties. A few aggregates were observed with the dispersed nanoparticles (Fig. 5). The observed aggregation of gefitinib-loaded NALM could have occurred during filtration sampling, in which particles were collected preferentially on previously collected particles by diffusion or interception and formed chainlike agglomerates known as dendrites (Przekop et al., 2003; Thomas et al., 2001).

A porous particle typically exhibits numerous voids that appear as regions of bright contrast in TEM images (Wei et al., 2010). In the gefitinib-loaded NALM TEM images, lack of such voids indicates non-porous NALM (Fig. 4). Furthermore, a layered structure with gradually decreasing contrast from the surface to the center of the NALM was observed (Fig. 4). It has been suggested that in the bright field imaging mode of TEM imaging, contrast formation occurs by sample electron occlusion and absorption. Thicker sample regions or those with a higher atomic number appear darker (Fultz and Howe, 2008). Gefitinib has a higher molecular mass (~447 g/mol) than the stearic acid lipid (~284 g/mol). Thus, it is possible that the observed gradual decrease in the contrast from the NALM surfaces to centers occurs because of varying drug enrichment extents in the different layers. The cores of the gefitinib-loaded NALM were brightest similar to hollow stearic acid NALM prepared in a pulse-heat aerosol reactor (Venkataraman and Pawar, 2011).

The observed layered structure in the TEM images (Fig. 4) can be explained based on the different molecular diffusion coefficients and relative solubility of gefitinib and stearic acid within the selected solvents. During droplet-to-particle formation from an evaporating solution drop, a receding drop surface causes a diffusional flux of solute molecules from the drop surface toward the center (Jayanthi et al., 1993). The relative timescales of solute diffusion are determined by the molecular diffusion coefficient, a function of molar volume (cc/mol). In the present study, the calculated timescales of the molecular diffusions of drug (gefitinib) and lipid (stearic acid) were similar (~1.6×10^{-5} s/cm) (Treybal, 1981). However, gefitinib has significantly lower solubility (≤0.1 mg/mL) than stearic acid (≥100 mg/mL) in the selected solvents. Thus, for a

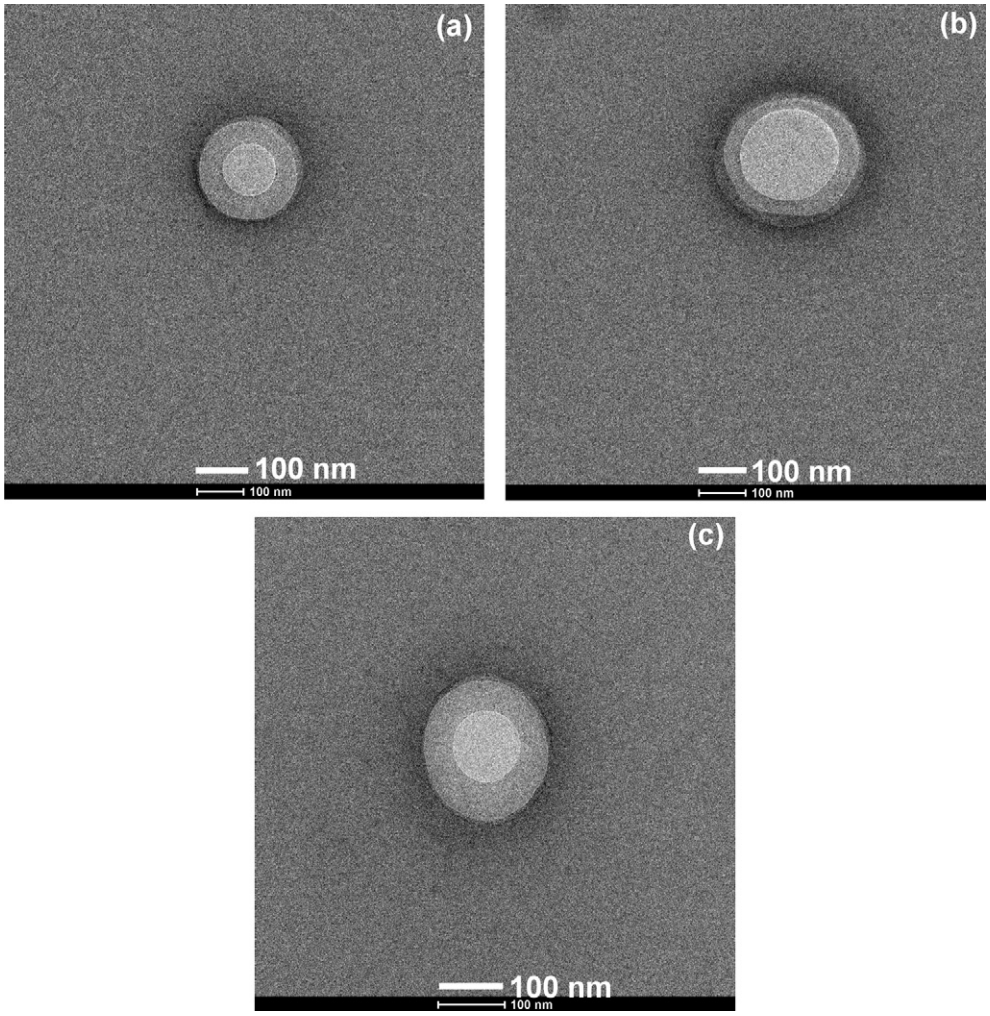

Fig. 4. Transmission electron microscopy (TEM) images of gefitinib-loaded nanoparticle aerosol lipid matrices (NALM) synthesized using gefitinib and stearic acid (1:4 w/w) solutions of (a) ethyl acetate (ETA), (b) chloroform (CHL), and (c) dichloromethane (DCM)

given diffusion timescale in an evaporating solution drop, gefitinib could reach saturation levels earlier than stearic acid and crystallizes around the surface of the developing particle (Duda, 1985). As observed under both TEM and SEM, gefitinib-loaded NALM were always spherical and non-porous, and they exhibited smooth surface properties and similarly layered structures.

3.3. Drug incorporation efficiency

Percent drug loading and entrapment efficiency were measured to understand drug incorporation extent and efficiency during the aerosol synthesis of drug-loaded NALM. The entire precursor solution containing 1:4 w/w of drug and lipid was atomized and the resulting particles were collected using fibrous filters. Overall collection efficiency of the fibrous filter, with a face velocity of 10.2 cm/s for particle diameters in the range of 50–500 nm, is reported to be ~74–98% (Hinds, 1999). This finding indicates that representative aerosol size distribution with a median mobility diameter of 123–132 nm was sampled. Thus, the initial drug to lipid mass ratio of the precursor solution was expected to be preserved in the collected gefitinib-loaded NALM.

The percent recovery of drug, expressed as entrapment efficiency (mass of drug in the NALM to the mass of drug used in the precursor solution), for all gefitinib-loaded NALM, synthesized at varying evaporation rates was $101 \pm 8\%$ w/w (Table 1). Entrapment efficiencies obtained by other lipid nanoparticle production methods, such as the solvent diffusion method and high-pressure homogenization, are about 50–70% w/w and 80–90% w/w, respectively (Alhaj et al., 2008; Hu et al., 2005; Paliwal et al., 2009).

The percent drug loading (mass of drug in the NALM to the mass of the collected NALM) for all of the gefitinib-loaded NALM synthesized at varying evaporation rates was $20 \pm 0.6\%$ w/w of drug and lipid. This finding indicates that the initial drug to lipid ratio (1:4 w/w) was preserved in the gefitinib-loaded NALM (Table 1). A higher mass per volume drug loading is crucial when high dose but reduced administration volume is required (Rabinow, 2004). Low drug loading capacities of 0.5–10% w/w drug to lipid are typically reported for lipid nanoparticles prepared using melt-emulsification techniques except for highly lipophilic cyclosporine and ubidecarenone, which have loading capacities of ~20–25% and 50% w/w, respectively (Muller et al., 2000; zur Muhlen et al., 1998). Constraining factors that limit the drug loading capacity in those lipid nanoparticles are low solubilization capacity of the molten lipids, crystalline polymorphic transformations of lipid matrix, and drug partitioning between the melted lipid and the aqueous dispersion medium (Bunjes, 2010; Muller et al., 2000). The drug loading obtained with gefitinib-loaded NALM (20% w/w) was higher than that obtained with lipid nanoparticles of similar sizes prepared using other methods. The differences among the drug loadings and drug entrapment efficiencies of the gefitinib-loaded NALM was not statistically significant ($p > 0.05$).

Table 1
Drug loading (% w/w) and drug entrapment (%) of gefitinib-loaded NALM synthesized using gefitinib and stearic acid (1:4 w/w) solutions of ethyl acetate (ETA), chloroform (CHL) and dichloromethane (DCM).

Lipid	Drug:lipid ratio	Drug loading (% w/w)	Drug entrapment (%)
SA + GF_ETA	1:4	20 ± 0.8	100 ± 1
SA + GF_CHL	1:4	21 ± 0.7	94 ± 1
SA + GF_DCM	1:4	20 ± 0.6	109 ± 16

3.4. Crystallinity of gefitinib-loaded NALM

Stearic acid nanoparticles containing gefitinib were prepared in an aerosol reactor using solvents having vapor pressures in the range of 12–57 kPa as demonstrated previously (Pawar and Venkataraman, 2011). To determine the crystalline state of lipids in gefitinib-loaded NALM, their PXRD and melting behaviors were analyzed vis-à-vis those of bulk stearic acid and a bulk mixture containing 1:4 w/w of drug to lipid (Figs. 6–7). Lower evaporation rates were observed to preserve the lipid crystallinity of stearic acid in gefitinib-loaded NALM. Gefitinib-loaded NALM synthesized at lower evaporation rates using the lower vapor pressure solvents ETA and CHL showed relatively larger peak areas and peak intensities in the PXRD diffractograms, implying higher lipid crystallinity (Table 2). Correspondingly, these NALM exhibited higher melting enthalpies in DSC thermograms, also indicating higher lipid crystallinity (Table 3). This trend was preserved across all evaporation rates. Differences in the estimated crystallinity of stearic acid using melting enthalpies (Venkateswarlu and Manjunath, 2004) were in the range of 31–52%. This finding indicates that the presence of gefitinib within the NALM did not affect control over the lipid crystallinity (Pawar and Venkataraman, 2011). Significant differences in the crystallinity of the lipid matrix were obtained, thereby enabling investigation of the related influence on drug release characteristics as discussed in the following section.

3.5. In vitro drug release

To investigate the influence of matrix crystallinity on drug release, the rate of in vitro drug release was measured from pure gefitinib nanoparticles and gefitinib-loaded NALM in PBS (pH 7.2) over a 10-day period. Rapid release was initially observed up to about 12 h, followed by a slow release (Fig. 8a and b). Compared to the control case of pure gefitinib nanoparticles, gefitinib-loaded NALM exhibited slower release, indicating the potential role of the lipid matrix in controlling drug release. Among the gefitinib-loaded NALM, slower drug release was obtained from particles with greater matrix crystallinity (Fig. 8a and b). This trend was preserved across the measured range of crystallinity (31–52%). The total cumulative percent of drug released (30–40%) from lipid matrices of higher lipid crystallinity was significantly smaller ($p < 0.05$) than

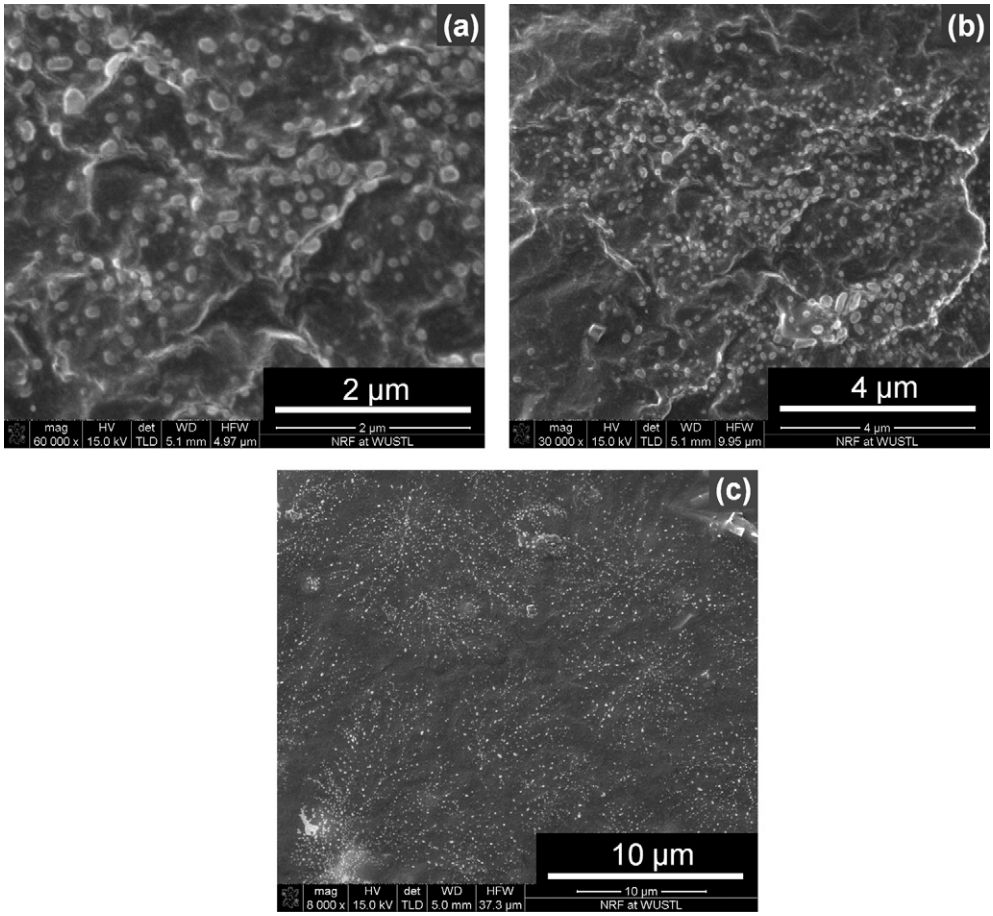

Fig. 5. Representative scanning electron microscopy (SEM) images of gefitinib-loaded nanoparticle aerosol lipid matrices (NALM) synthesized using gefitinib and stearic acid (1:4 w/w) ethyl acetate (ETA) solution

Table 2
PXRD diffractogram details (peak positions, d-spacings, relative intensities, peak area, and peak heights) of bulk stearic acid, bulk gefitinib, bulk mixture (1:4 w/w) of gefitinib and stearic acid (BM), and gefitinib-loaded NALM synthesized using gefitinib and stearic acid (1:4 w/w) solutions of ethyl acetate (ETA), chloroform (CHL) and dichloromethane (DCM).

Diffraction peaks	Bulk stearic acid	Bulk gefitinib	BM SA + GF	SA + GF ETA	SA + GF CHL	SA + GF DCM
Polymorphic form	C-form		C-form	C-form	C-form	C-form
Position 1	21.7	–	21.6	21.8	21.8	21.8
d-spacing (Ang.)	4.1	–	4.1	4.1	4.1	4.1
Rel. Inst (%)	100	–	73	31	39	19
Area (cts.[2Th])	4584	–	573	74	68	50
Height (cts)	5788	–	2140	125	127	99
Position 2	24.2	–	24.2	24.4	24.5	24.5
d-spacing (Ang.)	3.7	–	3.7	3.6	3.6	3.6
Rel. Inst (%)	14	–	52	6	6	6
Area (cts.[2Th])	442	–	437	14	13	12
Height (cts)	837	–	1616	23	20	28
Position 3	–	25.3	25.3	–	–	–
d-spacing (Ang.)	–	3.5	3.5	–	–	–
Rel. Inst (%)	–	64	3	–	–	–
Area (cts.[2Th])	–	159	37	–	–	–
Height (cts)	–	221	112	–	–	–
Position 4	–	26.4	26.5	–	–	–
d-spacing (Ang.)	–	3.4	3.4	–	–	–
Rel. Inst (%)	–	44	3	–	–	–
Area (cts.[2Th])	–	99	48	–	–	–
Height (cts)	–	185	143	–	–	–

the drug released (69%) from lipid matrices with lower lipid crystallinity (Fig. 8b).

Drug release from lipid nanoparticles has been linked to particle properties such as size, shape, drug loading, and release medium properties like pH (Subedi et al., 2009; Venkateswarlu and Manjunath, 2004; zur Muhlen et al., 1998). In the present study, particle size, shape, internal structure and drug loading of gefitinib-loaded NALM were relatively invariant (Sections 3.1–3.3). Uniform drug–lipid composition, the avoidance of surfactants, and constant composition of the release medium rationally precludes the changes in release rates because of drug–lipid interactions, varying lipid chain length, and the effects of surfactants and different media properties. However, the only significant difference found amongst the gefitinib-loaded NALM was in the measured degree of lipid crystallinity (Section 3.4). This finding indicates that the differing drug release rates obtained with gefitinib-loaded NALM synthesized at varying evaporation rates were influenced by the varying degrees of lipid crystallinity.

As a characteristic sustained drug release system, gefitinib-loaded NALM exhibited an initial rapid release followed by a prolonged sustained release (Fig. 8). An initial rapid release is required to attain the therapeutic range of drug concentration, followed by a prolonged release to maintain the same drug concentration for an extended period (Lachman et al., 1986). The initial rapid release from gefitinib-loaded NALM could be because of surface enrichment of the drug on the NALM (Section 3.2). The later prolonged release could possibly from the intermediate layer with medium darkness, where the drug could be molecularly dispersed among the crystalline interstitial spaces of lipid matrix. Intraparticle mass transfer is believed to result from a drug concentration gradient within the matrix. This could be because of both pore diffusion and solid diffusion (Perry et al., 1999). Since TEM imaging of gefitinib-loaded NALM in this study did not indicate porosity (Section 3.2), it can be surmised that pore diffusion may be neglected. Thus, solid diffusion is possibly the dominant mechanism of drug diffusion through the gefitinib-loaded NALM. The variation in NALM drug release rates could be linked to diffusivity differences through matrices with differing lipid crystallinities.

Studies focusing on solid diffusion across polymeric membranes and microparticles driven by a chemical potential gradient showed an exponential decrease in diffusion flux with increasing crystallinity (Bitter, 1984; Jeong et al., 2003). Drug molecule diffusion was suggested to occur solely through the amorphous fraction of the polymeric matrix, which was believed to form a coarse crystalline microstructure allowing rapid diffusion. However,

Table 3
Measured lipid crystallinity (melting point, melting enthalpy, and percentage lipid crystallinity) of bulk stearic acid, bulk gefitinib, bulk mixture (1:4 w/w) of gefitinib and stearic acid (BM), and gefitinib-loaded NALM synthesized using gefitinib and stearic acid (1:4 w/w) solutions of ethyl acetate (ETA), chloroform (CHL) and dichloromethane (DCM).

Lipid	Melting point (K)	Melting enthalpy ($J\,g^{-1}$)	Percent lipid crystallinity (%)[a]
Bulk SA	344 ± 0	213 ± 15	
Bulk GF	467 ± 0	136 ± 4	
BM SA + GF	343 ± 1	179 ± 7	100
SA + GF_ETA	335 ± 2	92 ± 19	52 ± 11
SA + GF_CHL	335 ± 1	72 ± 15	41 ± 9
SA + GF_DCM	335 ± 1	55 ± 9	31 ± 5

[a] The ratio of melting enthalpy of a processed lipid material to the melting enthalpy of standard value of stearic acid has been suggested as a percentage-crystallinity index (Venkateswarlu and Manjunath, 2004). In the present study the melting enthalpy of bulk mixture was taken as standard value to calculate percentage-crystallinity index.

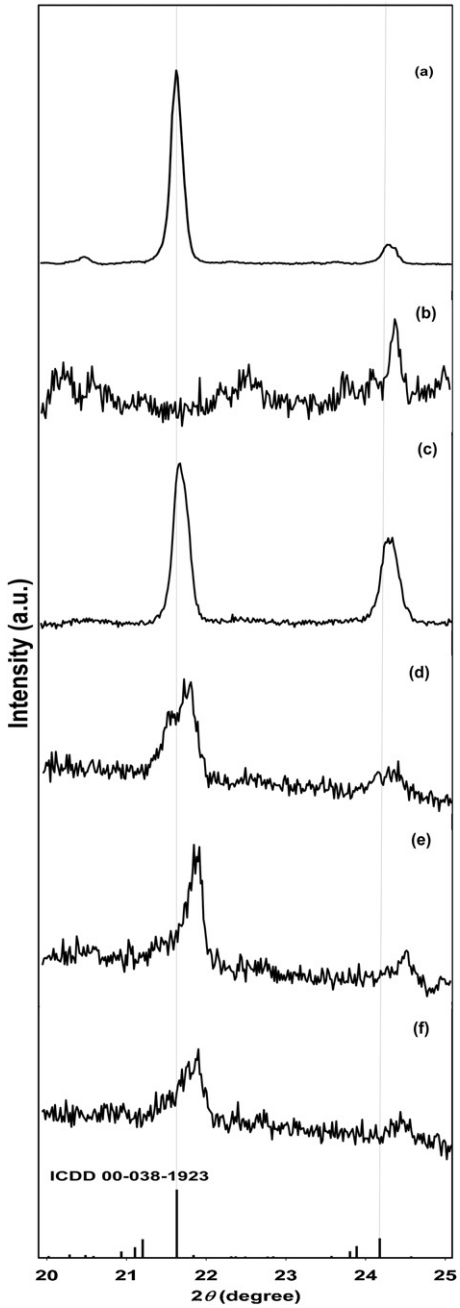

Fig. 6. Representative powder X-ray diffraction (PXRD) diffractograms of (a) bulk stearic acid, (b) bulk gefitinib, (c) a bulk mixture (1:4 w/w) of gefitinib and stearic acid, and gefitinib-loaded NALM synthesized using gefitinib and stearic acid (1:4 w/w) solutions of (d) ethyl acetate (ETA), (e) chloroform (CHL), and (f) dichloromethane (DCM).

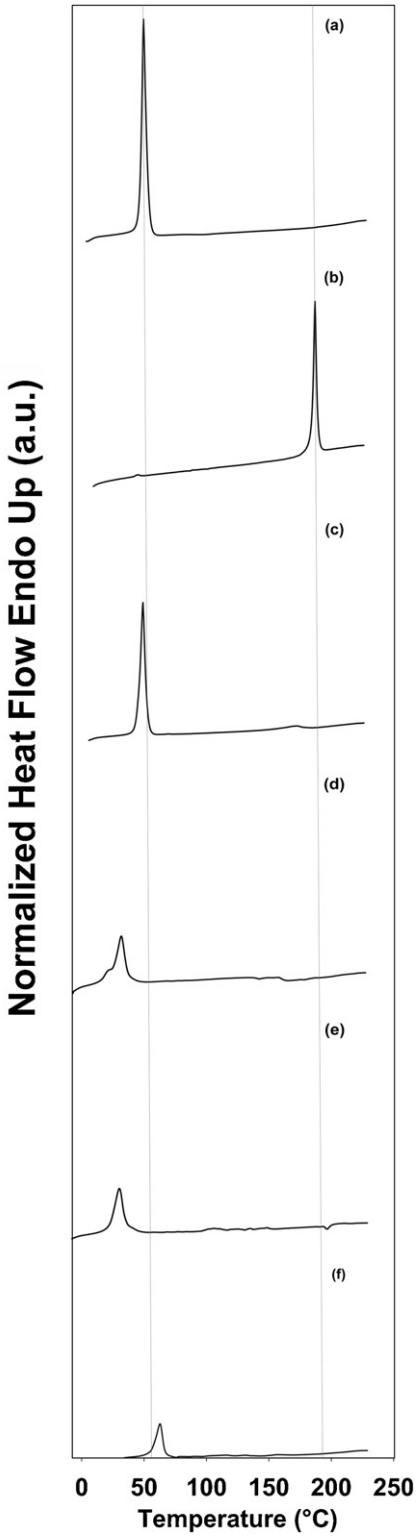

Fig. 7. Differential scanning calorimetry thermograms of (a) bulk stearic acid, (b) bulk gefitinib, (c) a bulk mixture (1:4 w/w) of gefitinib and stearic acid, and gefitinib-loaded nanoparticle aerosol lipid matrices (NALM) synthesized using gefitinib and stearic acid (1:4 w/w) solutions of (d) ethyl acetate (ETA), (e) chloroform (CHL), and (f) dichloromethane (DCM).

the crystalline regions of the matrices were indicated to effectively impede drug diffusion, resulting in a lower effective diffusion coefficient and a slower drug release (Arifin and Lee, 2006). Such a mechanism of slower diffusion through a more crystalline matrix may explain the slower drug release from the lipid matrices with higher degree of crystallinity demonstrated in this work (Fig. 8).

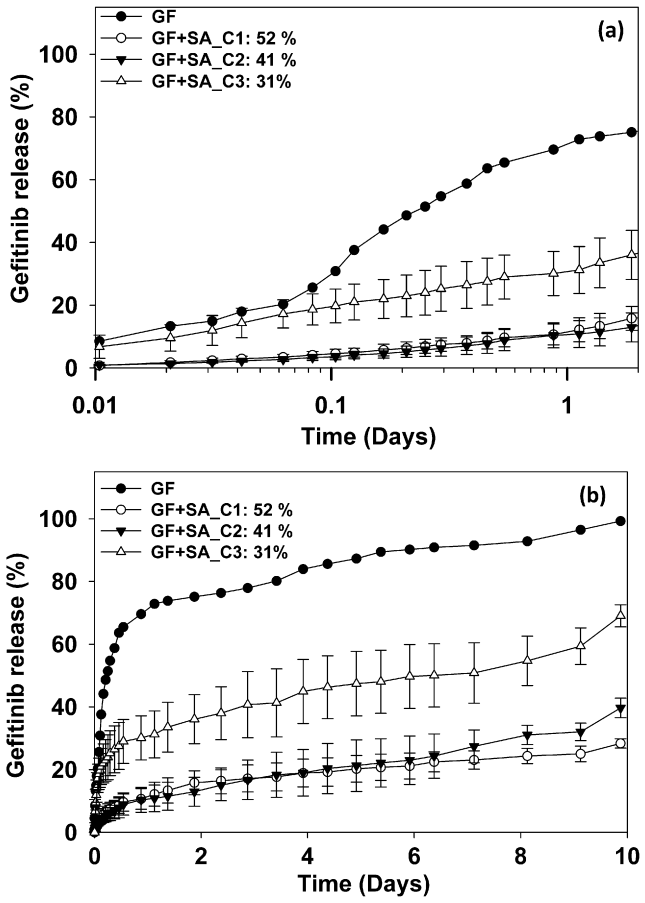

Fig. 8. Cumulative drug release, for a period of 2 days (a) and 10 days (b), from pure gefitinib nanoparticles (GF) and gefitinib-loaded nanoparticle aerosol lipid matrices (NALM) with crystallinity C1, C2, and C3 in descending order that were synthesized using gefitinib and stearic acid (1:4 w/w) solutions of ethyl acetate (ETA), chloroform (CHL), and dichloromethane (DCM), respectively.

4. Conclusions

The present study demonstrated that drug incorporation does not affect the crystalline properties of stearic acid lipid nanoparticles synthesized under controlled evaporation by the droplet-phase aerosol route. Gefitinib-loaded lipid matrices of sizes relevant to tumor or brain targeting applications were synthesized. Uniform and high drug entrapment that is essential for effective and predictable drug therapy was obtained. The drug to lipid ratio used in the precursor solution was preserved in the lipid matrices. Higher drug loading (~20% w/w) in the lipid nanoparticles was achieved using lipid solutions, than usually obtained using lipid melts (<5–10% w/w). Control over the crystallinity of gefitinib-loaded lipid matrices through differences in the evaporation rates of the precursor solvents was similar to the earlier demonstrated control with pure stearic acid nanoparticles. In vitro release studies demonstrated that, after an initial rapid release, gefitinib-loaded NALM allowed for extended drug delivery, possibly by intra-crystalline diffusion. The results suggest the determinant role of lipid crystallinity manipulated by differing evaporation rates on drug release rates from nanometer-sized lipid matrices. The present work reinforces the concept of droplet-phase aerosol synthesis of nanoparticle lipid matrices and control over their crystallinity obtained through differing evaporation rates of the precursor solvents for sustained drug release applications. The possible use of aerosol synthesis to produce nanoparticles using other crystalline lipids such as triglycerides can be explored with attention to constraints related to their lower crystallization tendencies and polymorphic transformations.

Acknowledgments

This work was supported by the Department of Science and Technology, Government of India, New Delhi (grant no. SR/S3/CE/54/2008); the Indian Institute of Technology, Bombay, Mumbai; and the Indo-US Science and Technology Forum, New Delhi. The authors also express appreciation to research engineer Kristy Wendt and the Nano Research Facility at the Washington University in St. Louis for assistance with the electron microscopy imaging.

References

Alhaj, N.A., Abdullah, A., Ibrahim, S., Bustamam, A., 2008. Tamoxifen drug loading solid lipid nanoparticles prepared by hot high pressure homogenization techniques. Am. J. Pharm. Toxicol. 3, 219–224.
Arifin, D.Y., Lee, L.Y.C.W., 2006. Mathematical modeling and simulation of drug release from microspheres: implications to drug delivery systems. Adv. Drug Deliv. Rev. 58, 1274–1325.
Bergman, E., Forsell, P., Persson, E.M., Knutson, L., Dickinson, P., Smith, R., Swaisland, H., Farmer, M.R., Cantarini, M.V., Lennernas, H., 2007. Pharmacokinetics of gefitinib in humans: the influence of gastrointestinal factors. Int. J. Pharm. 341, 134–142.
Bitter, J.G.A., 1984. Effect of crystallinity and swelling on the permeability and selectivity of polymer membranes. Desalination 51, 19–35.
Bunjes, H., 2010. Lipid nanoparticles for the delivery of poorly water-soluble drugs. J. Pharm. Pharmacol. 62, 1637–1645.
Bunjes, H., Westesen, K., Koch, M.H.J., 1996. Crystallization tendency and polymorphic transitions in triglyceride nanoparticles. Int. J. Pharm. 129, 159–173.
Chakraborty, S., Shukla, D., Mishra, B., Singh, S., 2009. Lipid – an emerging platform for oral delivery of drugs with poor bioavailability. Eur. J. Pharm. Biopharm. 73, 1–15.
Cohen, M.H., Williams, G.A., Sridhara, R., Chen, G., Pazdur, R., 2003. FDA drug approval summary: Gefitinib (ZD1839) (Iressa(R)) tablets. Oncologist 8, 303–306.
Duda, J.L., 1985. Molecular diffusion in polymeric systems. Pure Appl. Chem. 57, 1681–1690.
Fultz, B., Howe, J.M., 2008. Transmission Electron Microscopy and Diffractometry of Materials. Springer, Berlin Heidelberg.
Hinds, W.C., 1999. Aerosol Technology: Properties, behavior, and Measurement of Airborne Particles, 2nd ed. John Wiley & Sons, Inc.
Hu, F.Q., Jiang, S.P., Du, Y.Z., Yuan, H., Ye, Y.Q., Zeng, S., 2005. Preparation and characterization of stearic acid nanostructured lipid carriers by solvent diffusion method in an aqueous system. Colloids Surf. B: Biointerf. 45, 167–173.
Jayanthi, G.V., Zhang, S.C., Messing, G.L., 1993. Modeling of solid particle formation during solution aerosol thermolysis. Aerosol Sci. Technol. 19, 478–490.
Jeong, J., Lee, J., Cho, K., 2003. Effects of crystalline microstructure on drug release behavior of poly(ε-caprolactone) microspheres. J. Control. Release 92, 249–258.
Kheradmandnia, S., Vasheghani-farahani, E., Nosrati, M., Atyabi, F., 2010. Preparation and characterization of ketoprofen-loaded solid lipid nanoparticles made from beeswax and carnauba wax. Nanomed.: Nanotechnol. Biol. Med. 6, 753–759.
Kim, J.K., Park, J.S., Kim, C.K., 2010. Development of a binary lipid nanoparticles formulation of itraconazole for parenteral administration and controlled release. Int. J. Pharm. 383, 209–215.
Lachman, L., Lieberman, H.A., Kanig, J.L., 1986. The Theory and Practice of Industrial Pharmacy. Varghese Publishing House, Bombay.
Mehnert, W., Mader, K., 2001. Solid lipid nanoparticles – production, characterization and applications. Adv. Drug Deliv. Rev. 47, 165–196.
Muller, R.H., Mader, K., Gohla, S., 2000. Solid lipid nanoparticles (SLN) for controlled drug delivery – a review of the state of the art. Eur. J. Pharm. Biopharm. 50, 161–177.
Muller, R.H., Runge, S.A., Ravelli, V., Thunemann, A.F., Mehnert, W., Souto, E.B., 2008. Cyclosporine-loaded solid lipid nanoparticles (SLN®): drug-lipid physicochemical interactions and characterization of drug incorporation. Eur. J. Pharm. Biopharm. 68, 535–544.
Olbrich, C., Kayser, O., Muller, R.H., 2002a. Enzymatic degradation of Dynasan 114 SLN – effect of surfactants and particle size. J. Nanopart. Res. 4, 121–129.
Olbrich, C., Kayser, O., Muller, R.H., 2002b. Lipase degradation of Dynasan 114 and 116 solid lipid nanoparticles (SLN) – effect of surfactants, storage time and crystallinity. Int. J. Pharm. 237, 119–128.
Paliwal, R., Rai, S., Vaidya, B., Khatri, K., Goyal, A.K., Mishra, N., Mehta, A., Vyas, S.P., 2009. Effect of lipid core material on characteristics of solid lipid nanoparticles designed for oral lymphatic delivery. Nanomed.: Nanotechnol. Biol. Med. 5, 184–191.
Patra, C.R., Bhattacharya, R., Mukhopadhyay, D., Mukherjee, P., 2010. Fabrication of gold nanoparticles for targeted therapy in pancreatic cancer. Adv. Drug Deliv. Rev. 62, 346–361.

Pawar, A.A., Venkataraman, C., 2011. Droplet-phase synthesis of nanoparticle aerosol lipid matrices with controlled properties. Aerosol Sci. Technol. 45, 811–820.
Perry, R.H., Green, D.W., Maloney, J.O., 1999. Perry's Chemical Engineers' Handbook, 7th ed. McGraw-Hill.
Przekop, R., Moskal, A., Grado, L., 2003. Lattice-Boltzmann approach for description of the structure of deposited particulate matter in fibrous filters. J. Aerosol Sci. 34, 133–147.
Rabinow, B.E., 2004. Nanosuspensions in drug delivery. Nat. Rev. 3, 785–796.
Shetty, M., Pawar, A.A., Mehra, A., Venkataraman, C., 2011. Aerosol synthesis of lipid nanoparticles: relating crystallinity to simulated evaporation rates. Aerosol Sci. Technol., doi:10.1080/02786826.2011.648287.
Subedi, R.K., Kang, K.W., Choi, H., 2009. Preparation and characterization of solid lipid nanoparticles loaded with doxorubicin. Eur. J. Pharm. Biopharm. 37, 508–513.
Thomas, D., Penicot, P., Contal, P., Leclerc, D., Vendel, J., 2001. Clogging of fibrous filters by solid aerosol particles: experimental and modelling study. Chem. Eng. Sci. 56, 3549–3561.
Treybal, R.E., 1981. Mass-transfer Operations, 3rd ed. McGraw-Hill Book Company, Singapore, p 35.
Uner, M., Yener, G., 2007. Importance of solid lipid nanoparticles (SLN) in various administration routes and future perspectives. Int. J. Nanomed. 2, 289–300.
Venkataraman, C., Pawar, A.A., 2011. A Method and a System for Producing Thermolabile Nanoparticles with Controlled Properties and Nanoparticles Matrices Made Thereby. Indian Institute of Technology, Bombay India.
Venkateswarlu, V., Manjunath, K., 2004. Preparation, characterization and in vitro release kinetics of clozapine solid lipid nanoparticles. J. Control. Release 95, 627–638.
Wei, R., Pedone, D., Zurner, A., Doblinger, M., Rant, U., 2010. Fabrication of metallized nanopores in silicon nitride membranes for single-molecule sensing. Small 6, 1406–1414.
Westesen, K., Bunjes, H., Koch, M.H.J., 1997. Physicochemical characterization of lipid nanoparticles and evaluation of their drug loading capacity and sustained release potential. J. Control. Release 48, 223–236.
Wong, H.L., Bendayan, R., Rauth, A.M., Li, Y.Q., Wu, X.Y., 2007. Chemotherapy with anticancer drugs encapsulated in solid lipid nanoparticles. Adv. Drug Deliv. Rev. 59, 491–504.
zur Muhlen, A., Schwarz, C., Mehnert, W., 1998. Solid lipid nanoparticles (SLN) for controlled drug delivery – drug release and release mechanism. Eur. J. Pharm. Biopharm. 45, 149–155.